Desalination and Water Treatment
www.deswater.com
doi: 10.5004/dwt.2020.24864

174 (2020) 361–375
January

Uptake of crystal violet from water by modified Khalas dates residues

Muneera Abdullah Alfrhan[a], Hassan H. Hammud[a,*], Mohammed A. Al-Omair[a], Mervat A. El-Sonbati[b]

[a]*Department of Chemistry, College of Science, King Faisal University, Al-Hassa 31982, Saudi Arabia, emails: hhammoud@kfu.edu.sa (H.H. Hammud), mnalfrhan@kfu.edu.sa (M.A. Alfrhan), alomair@kfu.edu.sa (M.A. Al-Omair)*
[b]*Environmental Sciences Department, Faculty of Science, Damietta University, Egypt, email: mmossad5@du.edu.eg*

Received 7 March 2019; Accepted 5 September 2019

ABSTRACT

Removal of crystal violet dye (CV) from polluted water was studied by adsorption techniques. Adsorbents were prepared from waste residue available from syrup date industrial residue (SDIR). The SDIR from Khalas dates residue (KR) were modified by chemical treatment with formaldehyde to give KF, and with calcium chloride to give KC adsorbents. The characteristic of adsorbents was determined by Fourier-transform infrared spectroscopy (FTIR), scanning electron microscopy and thermogravimetric analysis. The optimum conditions were determined in batch experiments for the best uptake of crystal violet CV by adsorbents. The results showed that the adsorption data was well described by both Langmuir and Freundlich more than Temkin and followed the pseudo-second-order equation. Langmuir maximum capacity q (mg g^{-1}) for KF was found 144.49 mg g^{-1}, while it was 108.25 and 89.31 mg g^{-1} for KC and KR respectively. Thermodynamic and activated thermodynamic parameters were determined for the uptake of crystal violet and this study shows that the adsorption process is exothermic and spontaneous. The column breakthrough curve capacity was determined for the uptake of crystal violet by modified SDIR. It was found that Thomas and Yoon-Nelson column kinetics models describe best the experimental kinetic data, and the obtained capacity was 136.58 mg g^{-1} for KF and 89.11 mg g^{-1} for KC. The results prove that the SDIR (raw and treated) could be used as an effective and economical adsorbent for dye removal from wastewater.

Keywords: Adsorption; Crystal violet; Syrup date manufacture residue; Equilibrium; Kinetics; Thermodynamics

1. Introduction

Crystal Violet (CV), a triphenylmethane dye has been extensively used as a biological stain. It is used to hinder fungal growth in poultry feed and as a skin disinfectant in human beings [1]. The CV is also used for dyeing nylon, wool, plastics, gasoline, varnish, fat, oil and waxes [2,3].

The textile industry produces a large number of effluents and wastewater in the dyeing process which contains a massive amount of coloring agents and toxic undegradable substances. The textile wastewater with high CV dye has low dissolved oxygen since it contains high values of biochemical oxygen demand and chemical oxygen demand causing an environmental problem to reservoirs receiving the wastewater [4].

However, CV can cause skin and digestive tract inflammation and respiratory and kidney failure. It is also carcinogenic, it increases the risk of human bladder cancer [5,6]. The CV has considered as hazardous compound and its use was prohibited in the aquaculture and food industry. Several studies indicated that CV dye has carcinogenic and mutagenic effects in rodents and fishes [7], hinders seed

* Corresponding author.

germination, causes a decrease in root and shoot length of plant species and retards the activity of microbes contributing to soil fertility [8].

Thus, its remediation becomes the interest of many researchers. Adsorption is superior to other separation techniques because it is efficient, economically feasible and capable to separate a range of pollutants. Moreover, adsorbent materials from agricultural and food industry are abundant and have a very low cost. Also, chemical modification of biomass can give extra stability, durability and reuse for multiple cycles. It also give extra functional groups that increase the uptake capacity. Several biomass adsorbents were studied for CV adsorption. Examples are an aquatic plant "Water hyacinth" [3], citric acid modified rice straw [9], NaOH-modified rice husk [10], sugarcane bagasse [11], H_2SO_4 modified sugarcane bagasse [12], protonated watermelon [13]. sodium carbonate modified Bambusa tulda [14]

Thus, in the present work, we adopt adsorption techniques using "Khalas" Palm fiber waste residue from date syrup industries and its chemically modified form to efficiently remove the pollutant crystal violet from water. The following is undertaken to achieve the aim of the work: Chemical modification of date residues to prepare adsorbents, find the optimum condition for best uptake of crystal violet, test the ability of prepared adsorbents to uptake crystal violet from water using batch and column techniques.

2. Experimental setup

2.1. Chemicals and adsorbents

All chemicals used were of analytical reagent grade quality and were stored under dry conditions. Stock solutions of calcium chloride, sodium carbonate, sodium acetate, sodium hydroxide, and crystal violet dye were prepared by dissolving appropriate weight in double-distilled water. Formaldehyde (34.5%), hydrochloric acid (37%), and acetic acid (100%) were also diluted for further use. Crystal violet dye (CV) has a chemical formula $C_{25}H_{30}N_3Cl$, molar mass: 407.979 g mol^{-1}, CAS:548-62-9, and melting point 205°C [15].

The adsorbent Khalas dates residue (KR) from the manufacturing of Khalas syrup date by Al-Ahsa Food Industries Co. Ltd., (Hofuf, Saudi Arabia) is used as adsorbent of CV dye. KR was dried in an air-oven (model 30 Lab Oven) at 105°C for 22 h. The dried materials were grounded and sieved with 1 mm particle size sieve and then stored in an airtight container for further use and modification.

Modification of KR with calcium chloride $CaCl_2$:10.0 g of dried biomass of KR was treated with 400 ml of 0.2 M $CaCl_2$ solution at pH 5.5. The mixture was shaken for 12 h on a shaker incubator at 160 rpm, at 25°C. The biomass samples were filtered and washed with distilled water to eliminate extra calcium chloride and then dried in an air oven at 60°C for 24 h to give the adsorbent KC (KR modified with calcium chloride) [16,17].

Modification of KR with formaldehyde: 70 ml of formaldehyde (34.5%) and 135 ml of 0.1 M hydrochloric acid HCl solutions were added to 10.0 g of dried biomass KR. The mixture was stirred for 24 h. The biomass materials were then filtered, washed with double distilled water, then with 0.2 M sodium carbonate Na_2CO_3 solution, and finally with distilled water. The pre-treated materials were then dried at 60°C for 24 h to give the adsorbent KF (KR modified with formaldehyde) [17].

2.2. Batch mode adsorption study procedure

The isotherms experiments were performed by using 250 mL conical flasks containing 0.1 g adsorbent KR or its modified forms KF and KC and 100 ml crystal violet solution (pH = 5.5) in different initial concentrations (50, 100, 150, 200, 250, 300, 400, and 500 ppm) under the controlled temperature in a shaker incubator with constant speed of 160 rpm for 4 h. In a batch system, the effect of several parameters was studied such as temperature, sorbate concentration, sorbent dose, contact time and pH. At the desired time, the concentration of the dye (CV) in solution was obtained by using Ultraviolet-Visible (UV-VIS) Spectrophotometer at 590 nm, and the capacity (amount of dye (mg) removed by 1 g of adsorbent) can be calculated.

In the kinetics experiments, 0.1 g of adsorbent were placed into 250 Erlenmeyer flask containing 100 ml of 50 or 100 ppm dye solution. The mixture was shaken, and the remaining dye concentration was measured at 30 min intervals for a total of 240 min. The experiments were carried out at different temperatures to calculate the activated thermodynamics parameters.

2.3. Column mode adsorption study procedure

The dynamic adsorption system is important for studying the efficiency of a larger quantity of sorbent materials for removing sorbate from wastewater. The column study was carried using a Pyrex glass column of 30 cm length and 1.3 cm internal diameter. A 1 g of sorbent was packed into column then a standard solution of 200 ppm of CV was passed through the column with flow rate 1 ml min^{-1}. The effluent samples were collected at a different time and the dye concentration in the effluent was determined using a UV-VIS spectrophotometer. Initially, the concentration of dye in the effluent is negligible, then the concentration increases gradually until the column becomes saturated. This occurred when the concentration of the dye in the effluent equal the initial concentration of dye (200 ppm). For another adsorption cycle, the column was regenerated by 0.3 M HCl as an eluent solution with a flow rate of 1 ml min^{-1}. The column was then washed with distilled water until a pH = 5.5 to make sure the disposal of the remnants of acid before starting a new cycle.

3. Results and discussion

3.1. Adsorbent characterization

3.1.1. Fourier-transform infrared spectroscopy

Fourier-transform infrared spectroscopy (FTIR) spectra can give information about the nature of date residues functional groups responsible for the adsorption process. The spectra before and after modification are recorded for three types of date residues (Fig. 1). The data listed in Table 1 indicates that the adsorbent surface is complex. Infrared (IR)

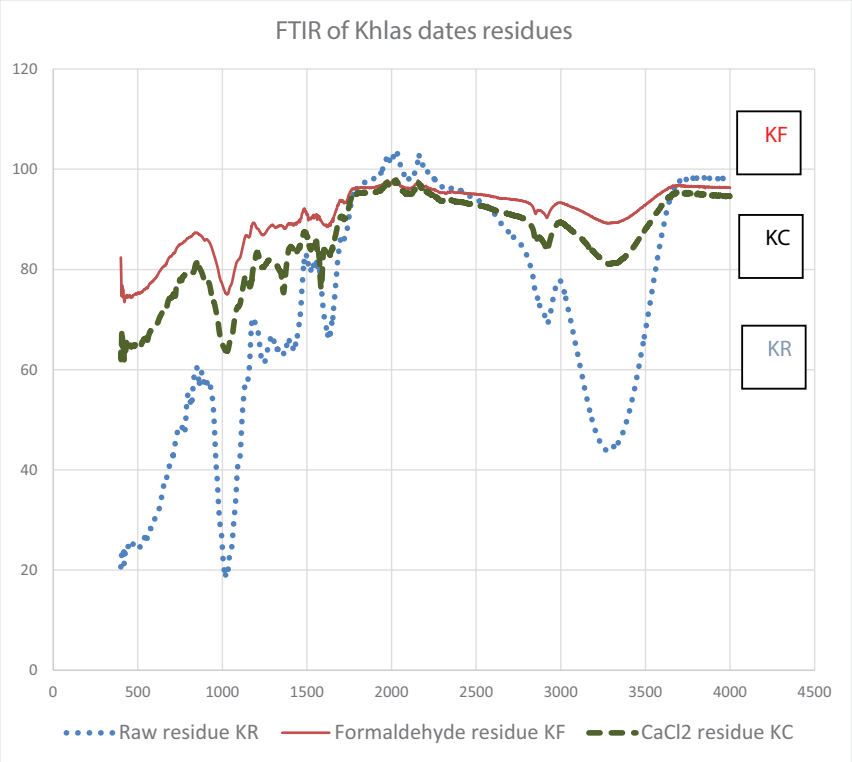

Fig. 1. FTIR spectra for KR raw, KF modified with formaldehyde, KC modified with calcium chloride before and KR*, KF*, KC* after CV adsorption.

absorption peaks of functional groups for cellulose, hemicellulose, and lignin indicate that date residues are capable of effective adsorption of dyes [18]. The broad stretching vibration peak of KR at about 3,306.69 cm^{-1} is due to the hydroxyl O–H group of cellulose and N–H group of amine. Carbonyl groups and aromatic rings show peaks at 1,718.68 [19] and 1,618.13 cm^{-1}. The strong C–O peak at 1,025.5 cm^{-1} confirms the existence of the cellulose structure. The peak at 1,244.25 cm^{-1} was due to C–N stretching vibration. Small peaks from 600 to 800 cm^{-1} indicate aromatic compounds with out of plane C–H stretching band modes.

IR peaks of KR after CV adsorption KR* shows shift compared to raw materials KR (Table 1). This shift confirms chemical interaction between dye and adsorbent surface, for example, the broad peak at 3,306.69 cm^{-1} for KR were shifted to higher wavenumber 3,339.98 cm^{-1}. The shifting of O–H, N–H and <C=O stretching vibrations indicates that hydroxyl, amine, and carbonyl groups were involved in CV adsorption. The new peaks at 1,583.5 and 1,362.6 cm^{-1} in KR* after dye loading, are due to aromatic and C–N groups characteristic of CV. Jain and Jayaram described that the hydroxyl group in the adsorbent and nitrogen atom in the amine group in CV were involved in adsorption through weak H-bond.

The FTIR spectra of KR modified with Formaldehyde KF Fig. 1 proved successful modification by formaldehyde

Table 1
FTIR spectral data for KR raw, KF modified with KF, KC modified with calcium chloride before and KR*, KF*, KC* after CV adsorption

	Stretching vibrations, wave number (cm^{-1})					
Functional group	KR	KR*	KF	KF*	KC	KC*
(O–H), (N–H)	3,306.69	3,339.98	3,294.8	3,314.68	3,334.91	3,340.94
(C–H)	2,919.36	2,916.61	2,918.13	2,917.64	2,917.3	2,918.42
	2,861.10	2,849.3	2,851.0	2,850.39	2,850.09	2,851.89
(C=O)	1,718.68	1,734.25	1,724.81	1,718.96	1,718.94	1,733.88
(C=C)	1,618.13	1,607.4	1,624.38	1,610.61	1,617.88	1,624.31
(C–N)	1,244.25	1,233.93	1,240.28	1,233.27	1,238.67	1,236.77
(C–O–C)	1,149.70	1,162.20	1,156.12	1,164.32	1,156.12	1,162.79
	1,025.50	1,029.25	1,029.25	1,027.20	1,027.26	1,027.16

due to shifting of peaks at 1,719 cm^{-1} belonging to <C=O group to around 1,724 cm^{-1}. The great shifting of IR wavenumbers between formaldehyde modified KR and formaldehyde modified KR after adsorption of CV KF* suggests chemical adsorption of dye with the involvement of hydroxyl, amino, and carboxyl groups. Also, new peaks appeared for KF* at 1,582.3; 1,355.8; and 1,162.5 cm^{-1} due to adsorbed CV dye (Fig. S1, Table 1). Functional groups peaks of KC at 3,334.91; 1,718.94; 1,617.88; and 1,156.12 cm^{-1} are shifted in $CaCl_2$ modified KR after adsorption of CV KC* to 3,340.94; 1,733.88; 1,624.31; and 1,162.79 cm^{-1} indicating occurrence of chemical interactions in the adsorption process. New peaks also appear at 1,584 and 1,362 cm^{-1} after adsorption of dye reflected the existence of aromatic ring and C–N group of CV (Table 1).

3.1.2. Scanning electron microscopy analysis

Scanning electron microscopy (SEM) is a primary instrument to characterize the surface morphology of adsorbent. The SEM images of KR, KF, and KC before and KR*, KF* and KC* after crystal violet adsorption were done using SEM (Jeol model 6360 LVSEM, USA), with a scale ranging from 10 to 100 mm. The results are shown in Fig. 2. All materials before adsorption have an irregular surface with some pores and cavities that enhance their ability for adsorption.

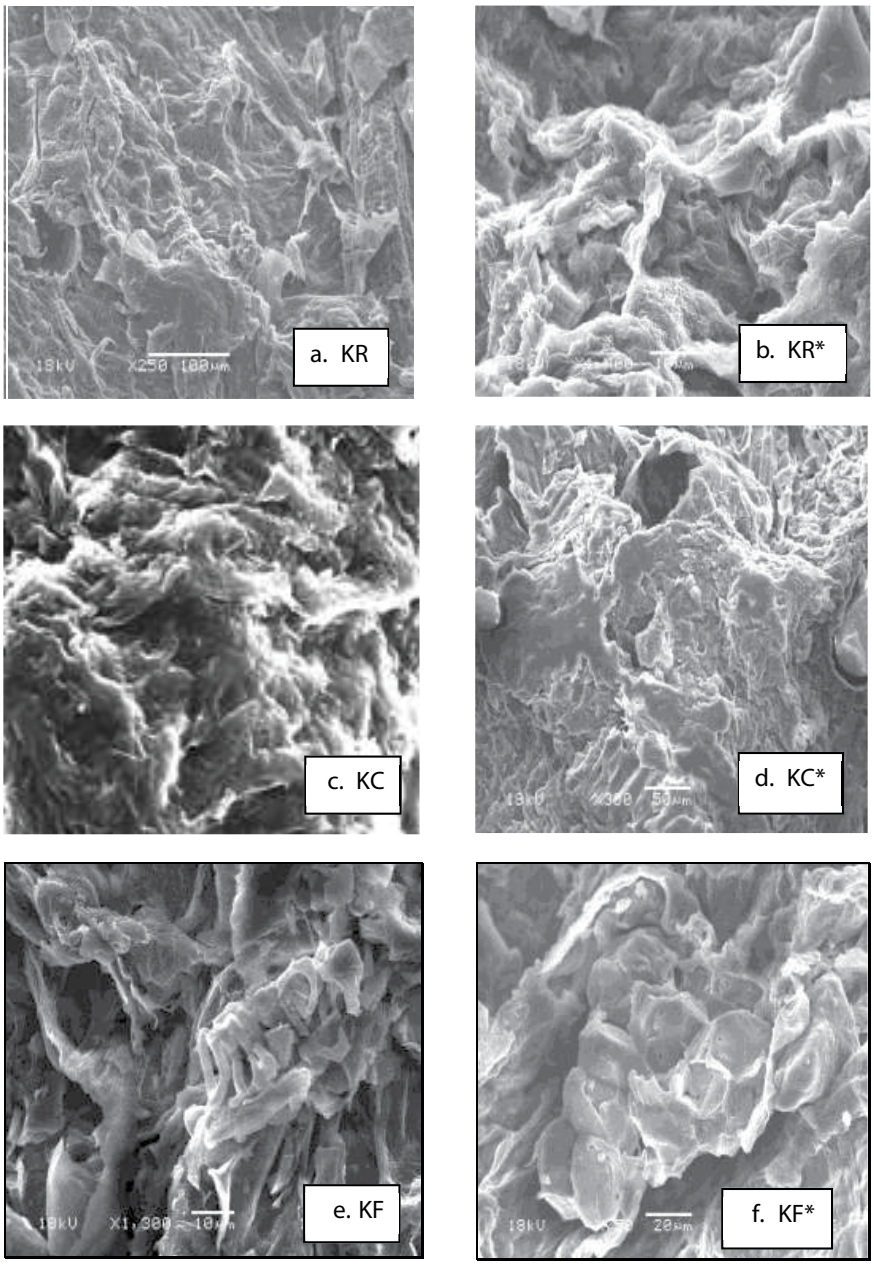

Fig. 2. SEM images (a,c,e) of KR raw, KC modified with calcium chloride, and KF modified with formaldehyde before adsorption, and (b,d,f) KR*, KC* and KF* after adsorption of CV.

Modified material KC and KF are more porous and thus have more potential for adsorption than raw material KR [21]. The surface morphology was changed in KF compared to KR. KF microstructure showed the formation of hollow rings as a result of the polymerization of raw materials by formaldehyde (Fig. 2). Obviously, after CV adsorption, the surface is fully covered by crystal violet (white spots) where the surface becomes less porous [22].

3.1.3. Thermogravimetric analysis

Thermogravimetric analysis (TGA) study of KF, KR and KC were done using Shimadzu TGA-50H (Japan) thermal analyzer under the nitrogen environment by heating from room temperature 25°C to 600°C at a heating rate of 15 min^{-1}. Several stages of degradation were obtained. The first stage of decomposition for KR occurred in the range from 25°C to 100°C which involved evaporation of moisture with weigh loss approximately (10.9%). Similar weight loss was reported by White et al. [23] for the evaporation of moisture from agriculture fibers. The second and last stage for KR occurred between 100°C–360°C corresponds to a loss of all organic materials with weight loss equal to 41.1%.

The first stage of loss of moisture (10.6%) of KF was followed by the second and third stages of mass loss. These occurred at 100°C–200°C and at 200°C–280°C respectively, because of degradation of cellulose and hemicellulose with mass loss (5.3%) and (8.6%) respectively [24]. The last decomposition between 280°C to 440°C (38.61%) is due to lignin since decomposition of lignin is more difficult then cellulose and hemicellulose [25].

While KC has almost no water loss in the first stage. The second stage occurred between 150°C–250°C with weight loss of 4.62% while the third stage occurred between 250°C–420°C with weight loss of 48%.

The last step which corresponds to major organic material loss has shifted to higher temperature values (250°C–440°C) in the case of KF and KC compared to (100°C–360°C) for KR. The increased thermal stability indicates that chemical modification of date residues has occurred.

3.2. Effect of different parameters on uptake of crystal violet by syrup date industrial residue

Effect of agitation time and initial concentration: For all solutions studied containing 0.1 g adsorbent in 100 ml CV dye solution (50, 100, 200, 300, 400, and 500 ppm) and shaken at 160 rpm, the % removal of CV by KF increases rapidly at initial times. However, it was observed that percent removal of crystal violet has little change after 180 min and at 240 min equilibrium is attained.

Effect of the mass of adsorbent: The effect of adsorbent dosage of KF on percent removal of crystal violet solution 100 ml with concentration 100 ppm at 25°C was investigated using the different mass of (0.03, 0.05, 0.07, 0.1, 0.15, and 0.2 g) shaken at 160 rpm for hours. The percent removal of crystal violet increase initially with an increase in the dose of KF due to an increase in surface area available of adsorbent sites, but after 0.1 g of adsorbent, no significant increment was noted in the removal of dye because all sites have been fully occupied [26]. Thus the optimum mass of KF was achieved at 0.1 g.

Effect of temperature: Adsorption process of crystal violet by different dates residues was studied at different temperatures (25°C, 30°C, 35°C, and 40°C) with a mixture of 0.1 g adsorbent into 100 ml (100 ppm) dye solution for 4 h. The results indicated that the percentage removal of dye decreases with increased temperature of the system and that the greatest % removal of KF 95% occurred at 25°C. This result suggests that the adsorption process is exothermic. A similar trend was reported by Chandra et al. [27] using activated carbon prepared from durian shell to remove methylene blue from aqueous solution. There are weakening in the bonds between the dye and the active sites of adsorbent as the temperature increase. Moreover at high temperature, the solubility of dye increases which increases the interaction between solute and solvent more than between solute and adsorbent [28].

3.3. Adsorption isotherms

Adsorption isotherms parameters describe the distribution of CV among two phases between solid and liquid phases, surface properties of adsorbent at equilibrium condition and adsorption capacity of the material. The linear and nonlinear isotherm models were applied at 25°C, 30°C, 35°C, and 40°C for Langmuir, Freundlich, and Temkin models [16,17]. The best model is the one with higher correlation coefficients R^2 and lower Chi-square test χ^2 and the sum of squared residuals (SSR) values for adsorption of CV by six types of syrup date industrial residue (SDIR) [16,17,29–32].

Linear and nonlinear Langmuir, Freundlich and Temkin constants and parameters for adsorption of CV by KR, KF, and KC at 303 K are listed in Table 2. While the results of the nonlinear isotherm model of KR modified with formaldehyde KF at different temperatures are presented in Table S1. The Langmuir linear plots for adsorption of CV onto KF and KC at 303 K are shown in Fig. 3. Temkin nonlinear plots of CV uptake by KC at 303 K are shown in Fig. S2. The Langmuir maximum capacity uptake q (mg g^{-1}) was found to decrease in the order KF, KC, and KR as such 144.49, 108.25, and 87.5 9 mg g^{-1} respectively, at 303 K. It was found that both Langmuir and Freundlich models are fitting the experimental data more than Temkin in most case, in terms of correlation coefficient close to 1.0 and low χ^2 and SSR values. Langmuir favors monolayer adsorption onto specific homogeneous sites, while Temkin describes multilayer adsorption onto heterogeneous sites of the adsorbent. Besides, it is observed from Table 2 that the values of R_L (separation factor) is between 0 and 1. This indicates favorable adsorption for overall results [33]. Similar results were obtained for adsorption of CV by treated ginger waste and date palm leaflets [34,35]. Moreover, the values of Freundlich constant (n) for all adsorbents are greater than 1, indicating strong adsorption between adsorbate and adsorbent at all studied temperatures [36]. Freundlich's constant K_F is greatest in the case of KF adsorbent.

Temkin equilibrium binding constant K_T (L g^{-1}) and heat of adsorption B_T are also highest for KF adsorbent, where the degree of adsorption for the Temkin model depends on the chemical nature and specific surface area of the adsorbent, and chemical nature, temperature, and concentration of the adsorbate. It was found that the capacity decreases with an

Table 2
Langmuir, Freundlich, and Temkin linear and non-linear model parameters for adsorption of 100 ml of crystal violet (50–500 ppm) by 0.1 g of KR, KF and KC at 303 K

Adsorbent	Langmuir			Freundlich			Temkin	
	Parameters	Linear	Non-linear	Parameters	Linear	Non-linear	Parameters	Non-linear
KR	q_{max} (mg g^{-1})	89.31	87.5 9	K_F (mg g^{-1}) × (L mg^{-1})$^{1/n}$	20.92	20.17	K_T (L g^{-1})	0.8911
	K_L (L mg^{-1})	0.0249	0.036	n	4.388	4.2	B_T (J mol^{-1})	13.76
	R^2	0.976	0.976	R^2	0.940	0.931	R^2	0.911
	χ^2	0.0926	16.98	χ^2	0.0072	28.70	χ^2	37.27
	SSR	0.3704	50.92	SSR	0.0288	115.10	SSR	149.09
	R_L	0.0743	0.0526					
KF	q_{max} (mg g^{-1})	138.73	144.49	K_F (mg g^{-1}) × (L mg^{-1})$^{1/n}$	34.38	35.26	K_T (L g^{-1})	1.57
	K_L (L mg^{-1})	0.0566	0.086	n	4.139	4.12	B_T (J mol^{-1})	22.41
	R^2	0.989	0.964	R^2	0.957	0.955	R^2	0.951
	χ^2	0.0146	90.65	χ^2	0.0187	83.07	χ^2	90.16
	SSR	0.0587	271.96	SSR	0.0751	332.28	SSR	360.64
	R_L	0.0341	0.0227					
KC	q_{max} (mg g^{-1})	109.36	108.25	K_F (mg g^{-1}) × (L mg^{-1})$^{1/n}$	20.98	21.09	K_T (L g^{-1})	0.442
	K_L (L mg^{-1})	0.0298	0.032	n	3.190	3.688	B_T (J mol^{-1})	20.29
	R^2	0.997	0.975	R^2	0.925	0.929	R^2	0.968
	χ^2	0.0072	21.33	χ^2	0.0159	60.59	χ^2	27.64
	SSR	0.0289	85.307	SSR	0.0638	242.38	SSR	110.57
	R_L	0.0628	0.0588					

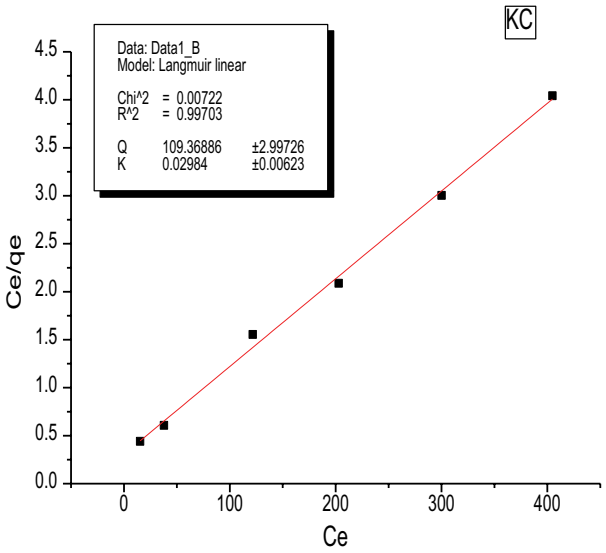

Fig. 3. Langmuir linear plots of uptake of CV by KC at 303 K. (0.1 g adsorbent, 100 ml of 100 ppm CV dye).

increase in temperature due to more dissolution of CV dye at high temperature (Table S1).

3.4. Adsorption kinetics

The kinetics of CV adsorption onto different types of syrup date residues were estimated according to two major common models, namely pseudo-first-order and pseudo-second-order. The plot of pseudo-second-order for KC and KR adsorbents at 25°C for 100 ppm CV is shown in Fig. 4. The values of capacities q_e and R^2 and rate constants k_1, k_2 for the two models obtained from kinetic plots, are presented in Table 3 for 100 and 50 ppm CV solutions.

Our experiments showed that for the concentrations studied 50 and 100 ppm at 25°C, the pseudo-second-order was fitted more than a pseudo-first-order kinetics model as indicated by high values of correlation coefficient R^2. Also, the theoretical capacity q_e calculated from pseudo-second-order is close to experimental capacity in many cases. As a result, the adsorption of CV by various types of date syrup residues followed the pseudo-second-order kinetics model. This suggests that chemical interaction occurred between sorbent and adsorbate. Similar results have been reported in the literature for the uptake of CV by palm kernel fiber, male flowers of the coconut tree and *Punica granatum* shell [37–39].

3.5. Adsorption mechanism

The experimental adsorption data of CV by KR are fitted to intra-particle diffusion plots to explain the mechanism responsible for the adsorption process. The obtained intra-particle diffusion constants and correlation coefficients are summarized in Table S2, [17,31].

All plots are double linear indicating that the mechanism of adsorption occurred in two stages: The first stage was very fast and happened in less than 15 min for all types of the adsorbent. This indicates that the dye diffuses into the

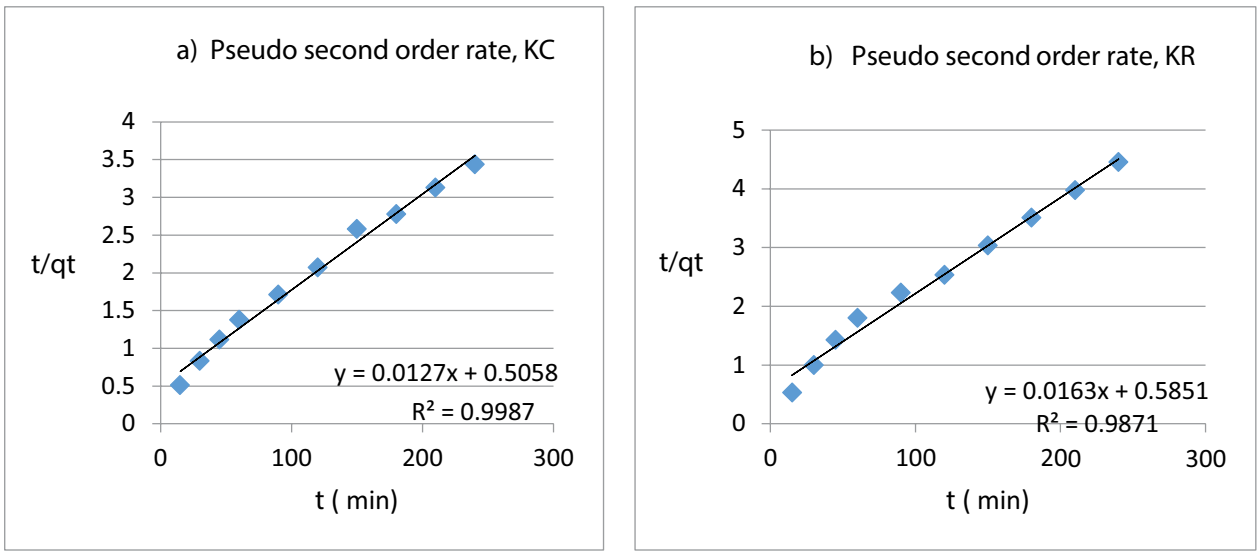

Fig. 4. Pseudo-second-order plots for the adsorption of 100 ml of CV dye (100 ppm) by 0.1 g of (a) KC and (b) KR adsorbents at 25°C.

Table 3
Pseudo-first-order and pseudo-second-order kinetics models parameters for the adsorption of CV 100 and 50 ppm solution (100 ml) onto 0.1 g of various types of date residue adsorbents at 25°C

CV dye (ppm)	Adsorbent	q_{exp}	Pseudo-first-order			Pseudo-second-order		
			q_e (mg g^{-1})	k_1 (min^{-1})	R^2	q_e (mg g^{-1})	k_2 (g mg^{-1} min^{-1})	R^2
100	KR	55.02	42.61	0.0140	0.981	61.35	0.00045	0.987
	KC	74.92	62.78	0.0080	0.975	78.74	0.00032	0.998
	KF	87.83	81.95	0.0092	0.924	88.49	0.00018	0.945
50	KR	34.84	22.22	0.0105	0.945	36.90	0.00084	0.984
	KC	47.86	23.99	0.0053	0.899	40.48	0.00102	0.973
	KF	43.25	57.74	0.0168	0.837	55.55	0.00030	0.981

external surface of adsorbent pores with strong interaction between (CV) and the surface of the adsorbent. The second stage is slower than the first due to the decrease in remaining dye concentration. In this rate-limiting step (second stage), the dye diffuses through the pores of the adsorbent. Both the first and second stages do not pass through the origin which indicates that the adsorption process is not only controlled by intraparticle diffusion [40]. The values of intraparticle diffusion rate constants in the first stage $K_{i,1}$ were higher than that of the second stage $K_{i,2}$ (Table S2). The reason could be pores blockage so that fewer sites are available for diffusion.

3.6. Thermodynamics parameters

The changes in thermodynamics parameters such as entropy (ΔS), enthalpy (ΔH), and Gibbs free energy (ΔG) for adsorption of CV onto different types of adsorbents were obtained from linear Van't Hoff plot and the result are reported in Table 4, [16–17,28–32]. The plots of lnK_e vs. 1/T for KF and KC are shown in Fig. S3, where K_e is the adsorption equilibrium constant.

The negative values of ΔG for all types of KR reflects that the adsorption process was feasible and spontaneous (Table 4). The decrease of ΔG negative values with an increase in temperature suggests that the adsorption process is more favorable at low temperatures [41]. The overall adsorption of CV onto all adsorbents indicates an exothermic process at all temperatures studied due to negative values of ΔH. Low enthalpy (<40 kJ mol^{-1}) suggests physical adsorption, while higher enthalpy (>40 kJ mol^{-1}) are characteristics for chemical adsorption. The obtained ΔS values were negative, which reflects increasing order at the solid-solution interface [42]. Similar phenomena were reported by Chakraborty et al. for adsorption of crystal violet onto NaOH-modified rice husk (NMRH), and for adsorption of CV onto rice straw modified with citric acid and for pineapple leaf powder [9,43].

3.7. Activation thermodynamic parameter

The calculated values of activation enthalpy (ΔH^*), activation entropy (ΔS^*), activation free energy (ΔG^*) and activation energy (E_a) for removal of CV by KR, KF and KC are presented in Table 4, [17,31]. Plots of lnk/T vs. 1/T to determine activation parameter and the plots of ln$K$ vs. 1/T to obtain activation energy for removal of CV by adsorbents KR and KF are shown in Fig. 5 and Fig. S4 respectively, where

Table 4
Thermodynamics and activated thermodynamic parameters for adsorption of 100 ml CV dye (100 ppm) by 0.1 g of different types of adsorbents at various temperatures

Adsorbent	T (K)	K_e	ΔG (kJ mol^{-1})	ΔH (ΔH^*) (KJ mol^{-1})	ΔS (ΔS^*) (J mol^{-1} K^{-1})	ΔG^* (kJ mol^{-1})	E_a (kJ mol^{-1})
KR	293	2.90	–2.80	–64.06	–205.57	102.23	17.59
	303	2.29	–1.77	(15.05)	(–292.57)	103.70	
	308	1.27	–0.75			105.16	
	313	0.89	0.28			106.62	
KF	293	19.08	–7.06	–79.07	–241.60	105.56	12.63
	303	8.50	–5.86	(10.09)	(–320.35)	107.16	
	308	6.70	–4.65			108.75	
	313	3.78	–3.44			110.36	
KC	293	2.99	–2.36	–14.35	–40.25	106.48	41.14
	303	2.27	–2.15	(39.91)	(–223.37)	107.59	
	308	2.09	–1.95			108.71	
	313	2.04	–1.75			109.83	

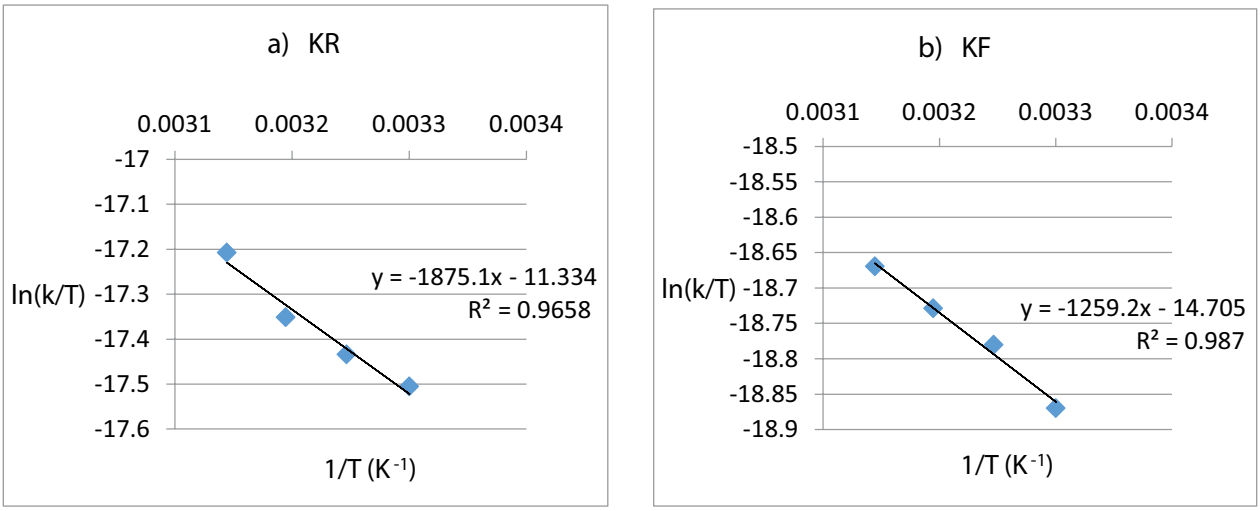

Fig. 5. Ln(K/T) vs. $1/T$ plot for the adsorption of 100 ml of CV dye (100 ppm) by 0.1 g of (a) KR and (b) KF.

K is the rate constant. As a result, the positive values of ΔG^* indicate that the adsorption process needs some energy to convert reactants onto transition products. Also positive and low values of (ΔH^*) at all temperatures suggest that the adsorption process is mostly entropy derived for all systems. A negative value of (ΔS^*) means that the entropy of reactants is more than the entropy of activated complex, which reflects that order in adsorption reaction increases during the formation of an activated complex between the adsorbent and adsorbate and involves associative mechanism [44]. E_a values obtained for all types of KR are reported in Table 4. At low E_a values in the range between 5 and 40 kJ mol^{-1} the adsorption mechanism is controlled by physical adsorption, while for the high value of E_a between 40 and 800 kJ mol^{-1} the adsorption mechanism is chemical adsorption [45]. In the case of adsorption of CV onto KR and KF adsorbents, E_a values were smaller than 40 kJ mol^{-1} indicating a physical mechanism for adsorption. While the mechanism is chemical in the case of KC

3.8. Column adsorption studies

3.8.1. Breakthrough curve

The column studied was packed with 1 g adsorbent dose, and eluted with 200 ppm initial concentration of dye concentration at a flow rate of 1 ml min^{-1}. Fig. 6 shows the breakthrough curves for two cycles of CV adsorption onto KF and KC. The column parameters, % removal and capacity (q_e) are calculated for the two cycles of CV from the breakthrough area method as shown (Table 5) [17,30,31]. Fig. S5 shows the plot of concentration of dye adsorbed C_{ad} (mg L^{-1}) vs. time (min) of KF and KC for each of cycle 1 and cycle 2, from which the area under the breakthrough curve was calculated (Table 5). Regeneration for column reuse was achieved with up to 99% efficiency by using dilute HCL 0.3 M.

Table 5 shows that the column filled with KF has the highest adsorption capacity 131.86 mg g^{-1} for the first cycle and that column saturation occurred after the passage of 800 ml

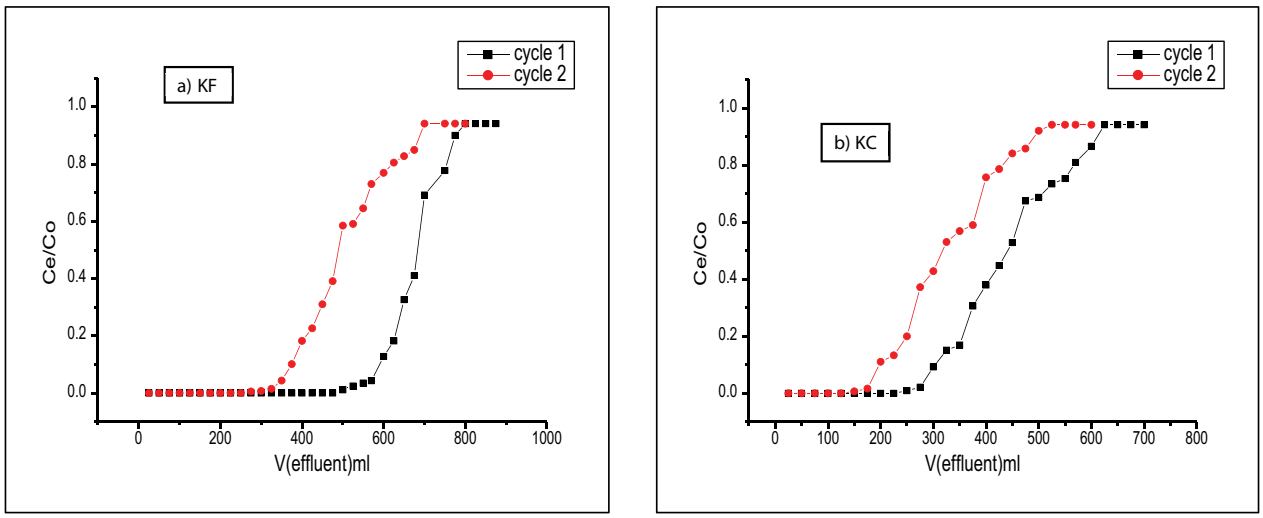

Fig. 6. Breakthrough curve for crystal violet uptake onto (a) KF and (b) KC respectively, (1 g adsorbent dose, 200 ppm initial dye concentration, flow rate 1 ml min^{-1}).

Table 5
% removal and capacity of column adsorption of CV by KF and KC. (1 g adsorbent dose, 200 ppm initial dye concentration, flow rate 1 ml min^{-1})

Adsorbent	Cycle	Area (mg min L^{-1})	q_{total} (mg)	M_{total} (mg)	% removal	q_e (mg g^{-1})	Column saturation time (min)
KC	Cycle 1	85,303.57	85.30	125	85.30	68.24	625
	Cycle 2	62,916.14	62.92	105	62.92	59.92	525
KF	Cycle 1	131,857.40	131.86	160	82.41	131.86	800
	Cycle 2	98,322.22	98.32	140	70.23	98.32	700

of crystal violet (200 ppm) solution with percent removal of 82.41%. While column study, using KC raw mixture material shows lower adsorption capacity (68.24 mg g^{-1}) for the first cycle. The exhaustion point of the column for the adsorption of CV by KC is obtained after the passage of the 625 ml CV solution.

3.8.2. Column kinetic model

In this study, Thomas, Yoon-Nelson and Yan et al. models were used to analyze column performance using the first cycle of column data for the adsorption CV by KF and KC [17,31,46]. The nonlinear regression was applied to plot adsorption data according to model equations in order to describe the behavior of adsorption of CV in a fixed bed column. For Thomas model, a plot of C_e/C_0 vs. time t (min) gave the values of Thomas constant and capacity K_T and q_T, where C_e (mg L^{-1}) is the concentration of adsorbate in the effluent, C_0 (mg L^{-1}) is the initial concentration of the adsorbate in the feed solution. Yoon-Nelson plot of C_e/C_0 vs. time t gave the values of Yoon-Nelson constant and capacity K_{YN} and q_{YN}. While from Yan et al. plot of C_e/C_0 vs. t, the values of Yan constant and capacity K_Y and q_Y were determined. The column kinetic parameter results for each model are presented in Table 6. Representative Thomas nonlinear model plots for the first cycle of adsorption of crystal violet by KF and KC are shown in Fig. 7.

All models fit well with the experimental breakthrough curves, having high values of R^2 and small error function (χ^2 and SSR) (Table 6). The column capacities obtained by Thomas and Yoon-Nelson nonlinear models were closer to the one obtained by the method of the area under the breakthrough curve and thus they describe best the behavior of adsorption of CV dye. While Yan et al. model showed much smaller capacity value and so it is less applicable.

3.9. Comparison of maximum adsorption capacity with other adsorbent material

The comparison of adsorption capacities of KR, KF, and KC in the present study with other low-cost adsorbents for the removal of crystal violet in batch and column model are shown in Table 7 [6,9,13,34,38,41,45,46–52]. The result indicates that KF with the highest capacities can be considered as a promising adsorbent to remove crystal violet from aqueous solution.

4. Conclusion

- Khalas Syrup date manufacture waste residues (SDIR) as agricultural waste, is a promising adsorbent for the uptake of CV dye from aqueous solution.
- The adsorption process of crystal violet shows significant improvement in sorption capacity with

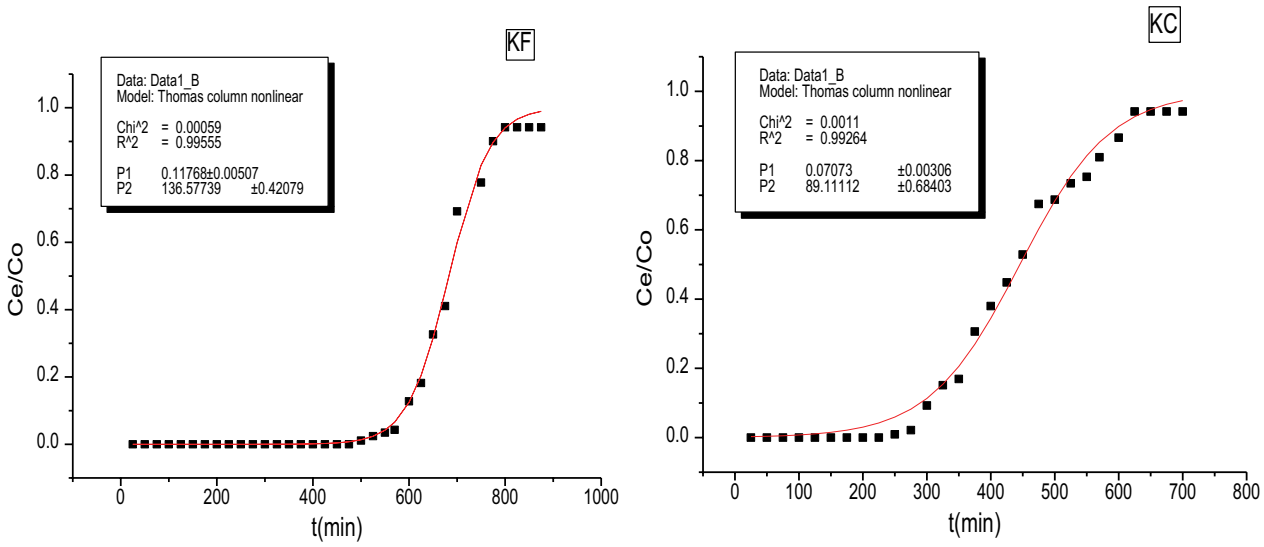

Fig. 7. Thomas nonlinear model plot for the first cycle of adsorption of crystal violet onto KF and KC, (1 g adsorbent dose, 200 ppm initial concentration of dye, flow rate 1 ml min^{-1}).

Table 6
Column kinetic parameters for adsorption CV (200 ppm) onto KF and KC with (1 g) packed column. (1 g adsorbent dose, 200 ppm initial dye concentration, flow rate 1 ml min^{-1})

Adsorbent	Thomas		Yoon-Nelson		Yan et al.	
	K_T (mL min^{-1} mg^{-1})	0.118	K_{YN} (min^{-1})	0.0235	K_Y (mL min^{-1})	8×10^{-5}
KF	q_T (mg g^{-1})	136.58	q_{YN} (mg g^{-1})	137.11	q_Y (mg g^{-1})	8.54
			τ(min)	682.28		
	R^2	0.996	R^2	0.996	R^2	0.996
	χ^2	6×10^{-4}	χ^2	6×10^{-4}	χ^2	5.0×10^{-4}
	SSR	0.0187	SSR	0.0187	SSR	0.0159
KC	K_T (mL min^{-1} mg^{-1})	0.0707	K_{YN} (min^{-1})	0.0142	K_Y (mL min^{-1})	3.0×10^{-5}
	q_T (mg g^{-1})	89.11	q_{YN} (mg g^{-1})	89.00	q_Y (mg g^{-1})	14.24
			τ(min)	445.55		
	R^2	0.992	R^2	0.992	R^2	0.996
	χ^2	0.0011	χ^2	0.0011	χ^2	5×10^{-5}
	SSR	0.0287	SSR	0.0287	SSR	0.0130

pretreated adsorbent with formaldehyde KF and calcium chloride KC.

- The adsorbents characteristics were examined by FTIR, SEM, and TGA which confirmed the successful dye adsorption onto different types of SDIR (KR, KF, and KC).
- In the batch experiment, the adsorption of crystal violet was found to increase in agitation time and reaches equilibrium at 240 min. However, the adsorption process is favorable at low temperatures.
- Both Langmuir and Freundlich isothermal models were best fitted to experimental data and perfectly describe the adsorption process more than the Temkin model based on the value of correlation coefficient (R^2) and function error values.
- The adsorption kinetics followed pseudo-second-order which indicates chemisorption. The intraparticle diffusion model is not the sole rate-limiting step.
- Thermodynamic study of crystal violet adsorption suggests that the adsorption process is exothermic and spontaneous due to the negative values of both enthalpy and free energy change.
- In a fix-bed column study, for uptake of CV by KF and KC date waste residues, Thomas and Yoon-Nelson column kinetics models describe the experimental kinetic data better than Yan et al model based on the values of correlation coefficient (R^2) and function error values. The calculated high capacity of CV adsorption is close to the value obtained from the breakthrough curve area method.
- Comparative study of adsorption capacity of syrup date manufacture residues and other adsorbent materials for the uptake of CV proves that the highest value of the adsorption capacity occurred with (CF) compared to other agricultural waste materials.

Table 7
Comparison of maximum adsorption capacity of KR, KF and KC with different adsorbents in batch mode and (column) mode

Adsorbent	Batch capacity (column capacity) (mg g^{-1})	References
Treated ginger waste	227.7	[34]
	(72.6)	
Grapefruit peel	254.16	[6]
Palm kernel fiber	78.9	[38]
NaOH-modified rice husk	44.87	[47]
Tea dust	175.4	[48]
Citric acid modified rice straw	80.91	[9]
	(77.185)	[41]
Jackfruit leaf powder	43.39	[49]
HCl-modified *Citrullus lanatus*	(61.49)	[45]
Rind	104.76	[13]
Citrullus lanatus rind	(46.68)	[50]
Water hyacinth	12.22	[51]
Date stone	90.89	[52]
KR	89.31	This study
KF	144.49	This study
	(136.58)	
KC	108.25	This study
	(89.11)	

- It can be concluded that SDIR (raw and treated) can be used as an available free low-cost preparation and local alternative for activated carbon to remove crystal violet from wastewater.
- The prepared modified date residues can be used to remove organic pollutants present in the wastewater.
- The availability of cheap date residues and its simple modification as well as the efficient adsorption method encourage their applications in industry.
- Prospect is to investigate the treatment of industrial wastewater using modified dates residues.

Acknowledgment

The financial support from the Deanship of Scientific Research (Project Number 160047) King Faisal University, is greatly acknowledged.

References

[1] V. Bonney, C.H. Browning, Sterilization of the skin and other surfaces by a mixture of crystal violet and brilliant green, Br Med J., 1 (1981) 562–563.
[2] W. Azmi, R.K. Sani, U.C. Banerjee, Biodegradation of triphenylmethane dyes, Enzyme Microb. Technol., 22 (1998) 185–191.
[3] M.R. Kulkarni, T. Revanth, A. Acharya, P. Bhat, Removal of Crystal Violet dye from aqueous solution using water hyacinth: equilibrium, kinetics and thermodynamics study, Resour.-Effic. Technol., 3 (2017) 71–77.
[4] M. Iqbal, M.Z. Ahmad, I.A. Bhatti, K. Qureshi, A. Khan, Cytotoxicity reduction of wastewater treated by advanced oxidation process, Chem. Int., 1 (2015) 53–59.
[5] A. Mittal, J. Mittal, A. Malviya, D. Kaur, V.K. Gupta, Adsorption of hazardous dye crystal violet from wastewater by waste materials, J. Colloid Interface Sci., 343 (2010) 463–473.
[6] A. Saeed, M. Sharif, M. Iqbal, Application potential of grapefruit peel as dye sorbent: kinetics, equilibrium and mechanism of crystal violet adsorption, J. Hazard. Mater., 179 (2010) 564–572.
[7] G.B. Michaels, D.L. Lewis, Sorption and toxicity of azo and triphyenylmethane dyes to aquatic microbial populations, Environ. Toxicol. Chem., 4 (2006) 45–50.
[8] S. Mani, R.N. Bharagava, Exposure to crystal violet, its toxic, genotoxic and carcinogenic effects on environment and its degradation and detoxification for environmental safety, Rev. Environ. Contam. Toxicol., 237 (2016) 71–104.
[9] S. Chowdhury, S. Chakraborty, P. Das (Saha), Adsorption of crystal violet from aqueous solution by citric acid modified rice straw: equilibrium, kinetics, and thermodynamics, Sep. Sci. Technol., 48 (2013) 1339–1348.
[10] S. Chowdhury, S. Chakraborty, P.D. Saha, Response surface optimization of a dynamic dye adsorption process: a case study of crystal violet adsorption onto NaOH-modified rice husk, Environ. Sci. Pollut. Res., 20 (2013) 1698–1705.
[11] S. Chakraborty, S. Chowdhury, P.D. Saha, Adsorption of crystal violet from aqueous solution onto sugarcane bagasse: central composite design for optimization of process variables, J. Water Reuse Desal., 2 (2012) 55–65.
[12] S. Chakraborty, S. Chowdhury, P.D. Saha, Batch removal of crystal violet from aqueous solution by H_2SO_4 modified sugarcane bagasse: equilibrium, kinetic, and thermodynamic profile, Sep. Sci. Technol., 47 (2012) 1898–1905.
[13] R. Lakshmipathy, N.C. Sarada, Adsorptive removal of basic cationic dyes from aqueous solution by chemically protonated watermelon (*Citrullus lanatus*) rind biomass, Desal. Wat. Treat., 52 (2014) 6175–6184.
[14] N. Laskar, U. Kumar, Adsorption of Crystal Violet from wastewater by modified Bambusa Tulda, KSCE J. Civ. Eng., 22 (2018) 2755–2763.
[15] N. Tahir, H.N. Bhatti, M. Iqbal, S. Noreen, Biopolymers composites with peanut hull waste biomass and application for Crystal Violet adsorption, Int. J. Biol. Macromol., 94 (2017) 210–220.
[16] H.H. Hammud, L. Fayoumi, H. Holail, El-Sayed M.E. Mostafa, Biosorption studies of methylene blue by mediterranean algae

carolina and its chemically modified forms. linear and nonlinear models' prediction based on statistical error calculation, Int. J. Chem., 3 (2011) 147–163.
[17] M. Hanbali, H. Holail, H. Hammud, Remediation of lead by pretreated red algae: adsorption isotherm, kinetic, column modeling and simulation studies, Green Chem. Lett. Rev., 7 (2014) 342–358.
[18] U.K. Garg, M.P. Kaur, V.K. Garg, D. Sud, Removal of nickel(II) from aqueous solution by adsorption on agricultural waste biomass using a response surface methodological approach, Bioresour. Technol., 99 (2008) 1325–1331.
[19] A.L. Cazetta, A.M.M. Vargas, E.M. Nogami, M.H. Kunita, M.R. Guilherme, A.C. Martins, T.L. Silva, J.C.G. Moraes, V.C. Almeida, NaOH-activated carbon of high surface area produced from coconut shell: kinetics and equilibrium studies from the methylene blue adsorption, Chem. Eng. J., 174 (2011) 117–125.
[20] S. Jain, R.V. Jayaram, Removal of basic dyes from aqueous solution by low-cost adsorbent: wood apple shell (*Feronia acidissima*), Desalination, 250 (2010) 921–927.
[21] Y. Kismir, A.Z. Aroguz, Adsorption characteristics of the hazardous dye Brilliant Green on Saklıkent mud, Chem. Eng. J., 172 (2011) 199–206.
[22] L.B.L. Lim, N. Priyantha, C.H. Ing, M.K. Dahri, D.T.B. Tennakoon, T. Zehra, M. Suklueng, *Artocarpus odoratissimus* skin as a potential low-cost biosorbent for the removal of methylene blue and methyl violet 2B, Desal. Wat. Treat., 53 (2015) 1–12.
[23] J.E. White, W.J. Catallo, B.L. Legendre, Biomass pyrolysis kinetics: a comparative critical review with relevant agricultural residue case studies, J. Anal. Appl. Pyrolysis, 91 (2011) 1–33.
[24] S. Ouajai, R.A. Shanks, Composition, structure and thermal degradation of hemp cellulose after chemical treatments, Polym. Degrad. Stab., 89 (2005) 327–335.
[25] X. Zhang, F. Wang, L.M. Keer, Influence of surface modification on the microstructure and thermo-mechanical properties of bamboo fibers, Materials (Basel), 8 (2015) 6597–6608.
[26] R. Ahmad, Studies on adsorption of crystal violet dye from aqueous solution onto coniferous pinus bark powder (CPBP), J. Hazard. Mater., 171 (2009) 767–773.
[27] T.C. Chandra, M.M. Mirna, Y. Sudaryanto, S. Ismadji, Adsorption of basic dye onto activated carbon prepared from durian shell: studies of adsorption equilibrium and kinetics, Chem. Eng. J., 127 (2007) 121–129.
[28] M. Alshabanat, G. Alsenani, R. Almufarij, Removal of crystal violet dye from aqueous solutions onto date palm fiber by adsorption technique, J. Chem., (2013) 1–6, http://dx.doi.org/10.1155/2013/210239.
[29] H.H. Hammud, I. Abbas, D. Al-khalili, Kinetics and thermodynamics of chromate and phosphate uptake by polypyrrole: batch and column studies, J. Inclusion Phenom. Macrocyclic Chem., 82 (2015) 395–405.
[30] H.H. Hammud, M.M. Chahine, B. El Hamaoui, Y. Hanifehpour, Lead uptake by new silica-carbon nanoparticles, Eur. J. Chem., 4 (2013) 432-440.
[31] H.H. Hammud, A. Shmait, N. Hourani, Removal of malachite green from water using hydrothermally carbonized pine needles, RSC Adv., 5 (2015) 7909–7920.
[32] I.I. Abbas, H.H. Hammud, H. Shamsaldeen, Calix[4]pyrrole macrocycle: extraction of Fluoride anions from aqueous media, Eur. J. Chem., 3 (2012) 156–162.
[33] X.-J. Xiong, X.-J. Meng T.-L. Zheng, Biosorption of C.I. Direct Blue 199 from aqueous solution by nonviable *Aspergillus niger*, J. Hazard. Mater., 175 (2010) 241–246.
[34] R. Kumar, R. Ahmad, Biosorption of hazardous crystal violet dye from aqueous solution onto treated ginger waste (TGW), Desalination, 265 (2011) 112–118.
[35] A. Sulyman, M. Namieśnik, A. Gierak, Adsorptive removal of aqueous phase crystal violet dye by low-cost activated carbon obtained from *Date palm* (L.) dead leaflets, Inżynieria i Ochrona Środowiska, 19 (2016) 611–631.
[36] C. Kannan, N. Buvaneswari, T. Palvannan, Removal of plant poisoning dyes by adsorption on Tomato Plant Root and green carbon from aqueous solution and its recovery, Desalination, 249 (2009) 1132–1138.
[37] S. Senthilkumaar, P. Kalaamani, C.V. Subburaam, Liquid phase adsorption of Crystal violet onto activated carbons derived from male flowers of coconut tree, J. Hazard. Mater., 136 (2006) 800–808.
[38] G.O. El-Sayed, Removal of methylene blue and crystal violet from aqueous solutions by palm kernel fiber, Desalination, 272 (2011) 225–232.
[39] M.B. Silveira, F.A. Pavan, N.F. Gelos, E.C. Lima, S.L.P. Dias, *Punica granatum* shell preparation, characterization, and use for crystal violet removal from aqueous solution, CLEAN - Soil Air Water, 42 (2014) 939–946.
[40] N.T. Abdel-Ghani, G.A. El-Chaghaby, E.M. Zahran, Pentachlorophenol (PCP) adsorption from aqueous solution by activated carbons prepared from corn wastes, Int. J. Environ. Sci. Technol., 12 (2015) 211–222.
[41] Z.K. Zhou, S.Q. Lin, T.L. Yue, T.-C. Lee, Adsorption of food dyes from aqueous solution by glutaraldehyde cross-linked magnetic chitosan nanoparticles, J. Food Eng., 126 (2014) 133–141.
[42] C. Varlikli, V. Bekiari, M. Kus, N. Boduroglu, I. Oner, P. Lianos, G. Lyberatos, S. Icli, Adsorption of dyes on Sahara desert sand, J. Hazard. Mater., 170 (2009) 27–34.
[43] S. Chakraborty, S. Chowdhury, P.D. Saha, Insight into biosorption equilibrium, kinetics and thermodynamics of crystal violet onto *Ananas comosus* (pineapple) leaf powder, Appl. Water Sci., 2 (2012) 135–141.
[44] T. Sismanoglu, A. Ercag, S. Pura, E. Ercag, Kinetics and isotherms of dazomet adsorption on natural adsorbents, J. Braz. Chem. Soc., 15 (2004) 669–675.
[45] T.S. Anirudhan, P.G. Radhakrishnan, Thermodynamics and kinetics of adsorption of Cu(II) from aqueous solutions onto a new cation exchanger derived from tamarind fruit shell, J. Chem. Thermodyn., 40 (2008) 702–709.
[46] H.H. Hassan, B. El Hamaoui, N.H. Noubani, X.L. Feng, Z.-S. Wu, K. Müllen, K. Ayub, Carbon-cobalt nanostructures as an efficient adsorbent of malachite green, Nanosci. Nanotechnol.-Asia, 8 (2018) 263–280.
[47] S. Chakraborty, S. Chowdhury, P.D. Saha, Adsorption of Crystal Violet from aqueous solution onto NaOH-modified rice husk, Carbohydr. Polym., 86 (2011) 1533–1541.
[48] M.M.R. Khan, M.W. Rahman, H.R. Ong, A.B. Ismail, C.K. Cheng, Tea dust as a potential low-cost adsorbent for the removal of crystal violet from aqueous solution, Desal. Wat. Treat., 57 (2016) 14728–14738.
[49] P.D. Saha, S. Chakraborty, S. Chowdhury, Batch and continuous (fixed-bed column) biosorption of crystal violet by *Artocarpus heterophyllus* (jackfruit) leaf powder, Colloids Surf., B, 92 (2012) 262–270.
[50] K.S. Bharathi, S.P.T. Ramesh, Fixed-bed column studies on biosorption of crystal violet from aqueous solution by *Citrullus lanatus rind* and *Cyperus rotundus*, Appl. Water Sci., 3 (2013) 673–687.
[51] K. Murali, P. Arunkumar, J. Kanmani, S. Kurunthasala Prabu, N. Jayaganesh, Removal of Crystal violet dye using water hyacinth, Int. J. Eng. Res. Modern Educ., Special Issue, (2017) 139–141.
[52] N. El Messaoudi, M. El Khomri, S. Bentahar, A. Dbik, A. Lacherai, Removal of crystal violet by biosorption onto date stones, Sci. Study Res. Chem. Chem. Eng. Biotechnol. Food Ind., 17 (2016) 151–167.

Supplementary information

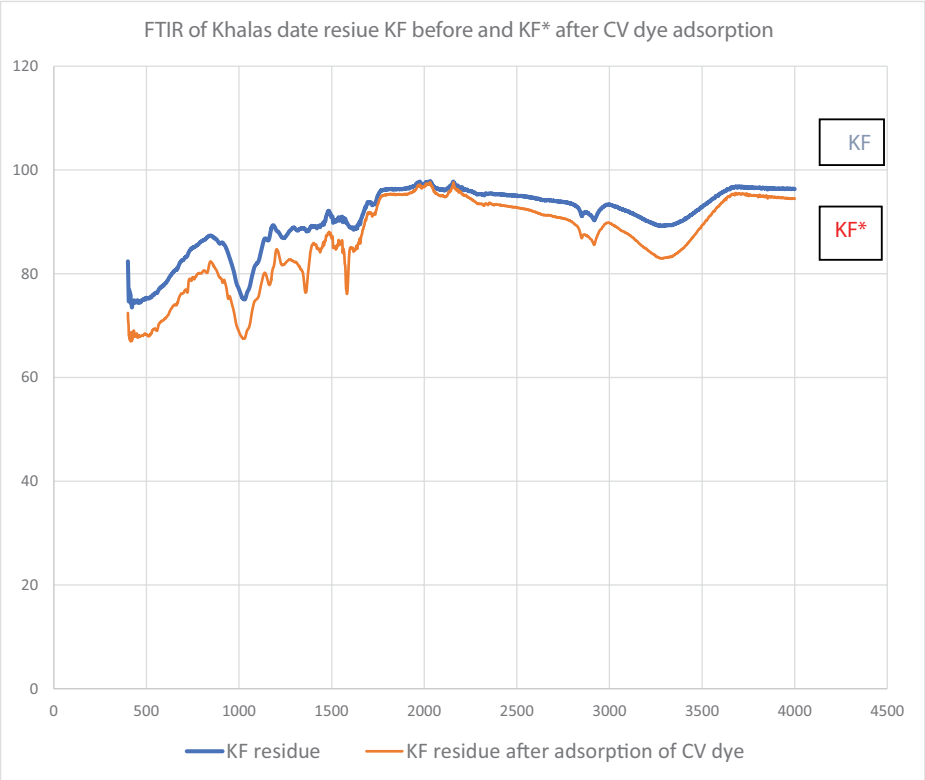

Fig. S1. FTIR spectrum of formaldehyde modified residues KF before and KF* after adsorption of CV dye.

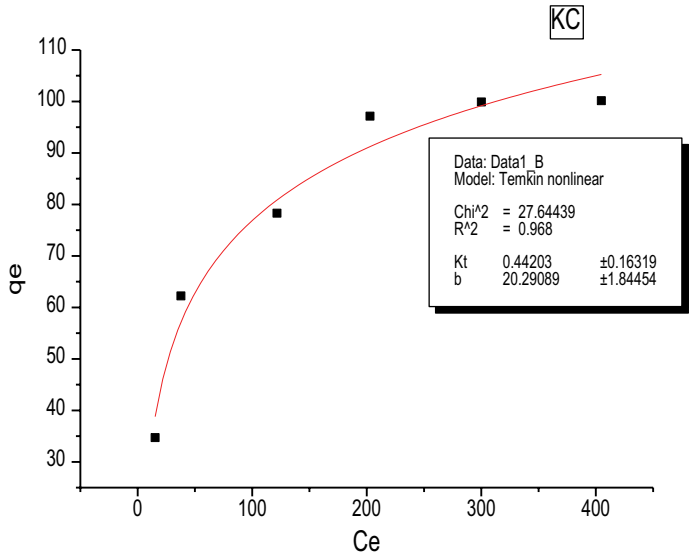

Fig. S2. Temkin nonlinear plots for the uptake of crystal violet 100 ml (50–500 ppm) by 0.1 g of CV dye by KC at 303 K.

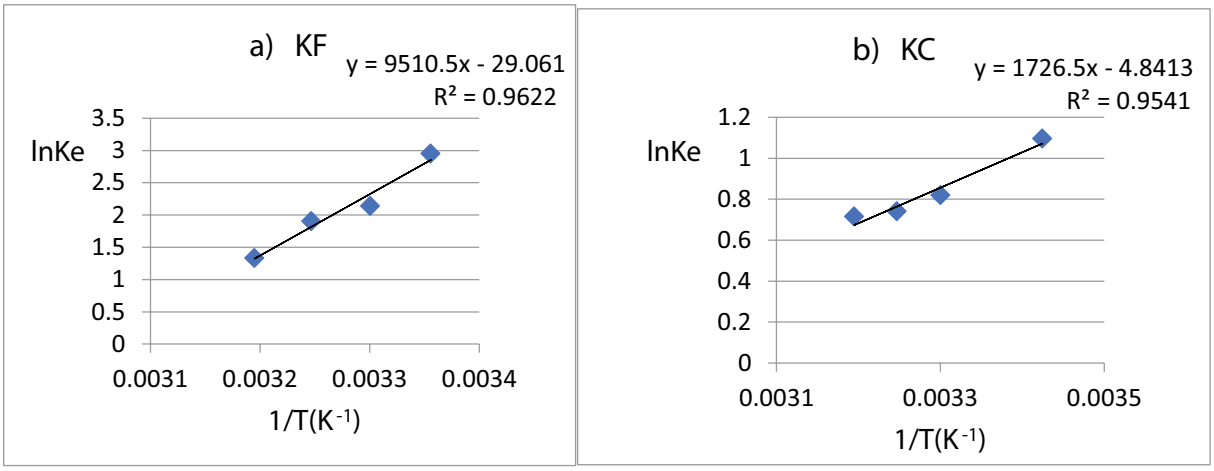

Fig. S3. LnK_e vs. 1/T Plots for the adsorption of CV dye (100 ml and 100 ppm) onto KF and KC.

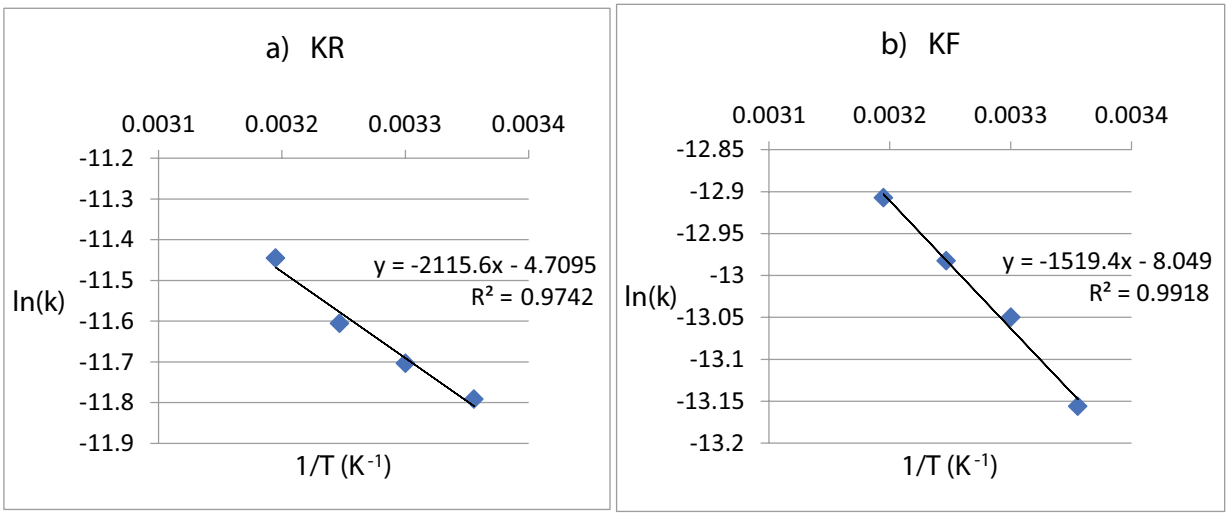

Fig. S4. LnK vs. 1/T plot for the adsorption of CV dye (100 ml and 100 ppm) by 0.1 g (a) KR and (b) KF.

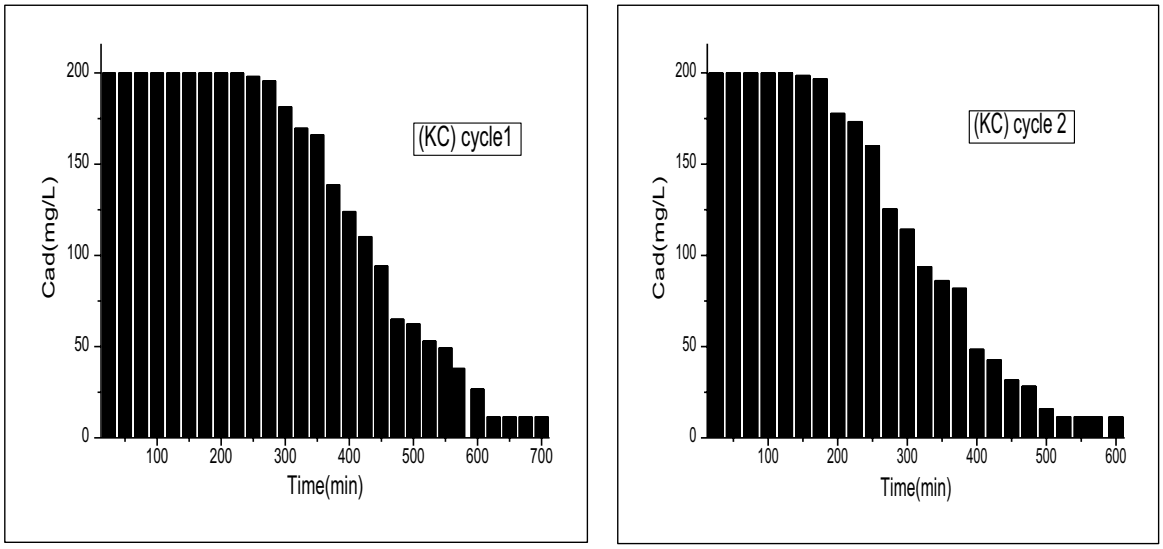

Fig. S5. Plots of C_{ad} against time (min) for KC of cycle 1 and cycle 2. (1 g adsorbent dose, 200 ppm initial dye concentration, flow rate 1 ml min^{-1}).

Table S1
Nonlinear isotherm models for the adsorption of 100 ml of crystal violet (50–500 ppm) by 0.1 g of KR modified with formaldehyde KF at different temperatures

	Langmuir			Freundlich			Temkin		
T (K)	q_m	K	R^2	K_F	n	R^2	K_T	B_T	R^2
298	151.28	0.083	0.921	40.10	4.28	0.984	2.79609	21.754	0.977
	χ^2	SSR	R	χ^2	SSR	R	χ^2	SSR	R
	223.79	671.38	0.960	18.368	91.84	0.994	38.530	192.65	0.988
303	q_m	K	R^2	K_F	n	R^2	K_T	B_T	R^2
	144.49	0.086	0.964	35.256	4.12	0.955	1.56988	22.412	0.9518
	χ^2	SSR	R	χ^2	SSR	R	χ^2	SSR	R
	90.65	271.96	0.981	83.07	332.28	0.977	90.1608	360.64	0.975
308	q_m	K	R^2	K_F	n	R^2	K_T	B_T	R^2
	142.12	0.046	0.964	28.36	3.709	0.911	0.83733	23.459	0.9124
	χ^2	SSR	R	χ^2	SSR	R	χ^2	SSR	R
	83.81	251.45	0.982	158.85	635.43	0.954	157.482	629.92	0.9552
313	q_m	K	R^2	K_F	n	R^2	K_T	B_T	R^2
	114.28	0.0733	0.931	36.78	5.139	0.828	2.10757	17.357	0.873
	χ^2	SSR	R	χ^2	SSR	R	χ^2	SSR	R
	65.04	260.16	0.964	161.98	647.92	0.910	119.046	476.18	0.9348

Table S2
Intraparticle diffusion rate constants and parameters for the adsorption of CV 100 ppm solution (100 ml) by 0.1 g KR, KF, and KC at 25°C

Adsorbent	$K_{i,1}$ (mg (g^{-1} $min^{-1/2}$))	I_1 (mg g^{-1})	R^2	$K_{i,2}$ (mg (g^{-1} $min^{-1/2}$))	I_2 (mg g^{-1})	R^2
KR	2.65	15.17	0.965	0.0518	53.05	1
KC	3.57	16.61	0.987	0.2238	66.27	1
KF	4.79	4.23	0.973	0.337	75.05	0.999